A&A 398, 353–361 (2003)
DOI: 10.1051/0004-6361:20021610

Astronomy & Astrophysics

Icy grains as a source of CO in comet 29P/Schwassmann-Wachmann 1

M. Gunnarsson⋆

Astronomiska Observatoriet, Box 515, 75120 Uppsala, Sweden

Received 22 March 2002 / Accepted 5 November 2002

Abstract. A model of micron-sized icy grains is used to simulate the behaviour of solid material ejected from comet 29P/Schwassmann-Wachmann 1, which resides at ∼6 AU from the Sun. It is demonstrated that a population of grains composed primarily of water ice can release their ice content on timescales of order 10^6 s. This justifies the idea that icy grains can serve as an extended source of more volatile species, as was assumed when evidence for a coma source of CO was found in radio observations of this comet. The model also predicts short lifetimes for the icy grains inside 3 AU from the Sun, removing the extended appearance of the CO production at smaller heliocentric distances, as seen in comet Hale-Bopp. A grain population sublimating in a time interval similar to that derived for the coma source of CO in comet 29P/Schwassmann-Wachmann 1 must have most of its mass concentrated to small (with radii <5 μm) or porous grains. Those grains must carry a significant ice content, with an refractory to ice ratio of less than ∼30%. By introducing continuous grain fragmentation the extended source activity can be reproduced for a grain population that includes larger particles. This would call for grains to split into smaller pieces on a timescale of $\sim 5 \times 10^5$ s.

Key words. comets: individual: 29P/Schwassmann-Wachmann 1 – dust

1. Introduction

The prevailing idea about how comets are built is that they are composed of a porous mixture of ice and dust. In an active comet icy dust grains – or "dirty" ice grains – are assumed to follow the gaseous outflow. This assumption was made even before icy grains were actually detected in a comet, since they were needed to explain various observed phenomena (Hanner 1981). However, detection of such grains is difficult since their lifetimes are short at the heliocentric distances where comets are normally observed to be active. Inside around 2 AU the icy component sublimates before the grains have filled a significant part of the observed coma, leaving only the refractory part. For a chance to detect icy grains in a comet, it must be observed when being active at larger heliocentric distances. In comet Hale-Bopp, when between 4.6 and 2.8 AU, evidence of water ice in the coma was found by ISO observations done in 1996 (Lellouch et al. 1998; Grün et al. 2001).

Comet 29P/Schwassmann-Wachmann 1 (hereafter SW1) has been studied in a millimeter-wave observing campaign carried out at the Swedish-ESO Submillimeter Telescope (SEST). In 1996, indications were found that carbon monoxide is being produced from a coma source (Festou et al. 2000, hereafter Paper I). Further observations in 1998 confirmed this, and the basic character of the extended source was determined. The CO-producing material was found to have its activity localized outside a distance of $1-2 \times 10^5$ km from the nucleus, corresponding to a travel time of order $2-4 \times 10^6$ s (Gunnarsson et al. 2002, hereafter Paper II).

The mechanism behind the extended source was found to be consistent with CO being released from solid particles ejected from the nucleus by outgassing confined to a region near the subsolar point. Comet SW1 resides at a steady heliocentric distance around 6 AU, where sublimation of water ice in a cometary nucleus is inefficient. The released particles are thus assumed to be "icy", i.e. consist of, or carry a component of H_2O ice with inclusions of other, more volatile species, including CO.

If CO is contained in initially amorphous H_2O ice, and this ice is subject to gradual heating to temperatures above 100 K, the CO release rate has two distinct peaks (Bar-Nun & Kleinfeld 1989). These two peaks correspond to crystallization of the ice, which is assumed to be the driving mechanism behind the nuclear outgassing and expulsion of solid material, and sublimation of the ice, when everything contained in it must be released.

The limiting distance of order 10^5 km found in Paper II should be seen as the inside radius of a shell-like cloud of CO-producing material. Inside this radius the solid material must have a low level of activity, and outside of this radius, the bulk of the CO content is released. While the observations cannot provide an outside radius of the region of activity, it must also be assumed that most of the available CO is released not too long after the "onset" of activity, giving an activity region of

⋆ e-mail: marcus@astro.uu.se

limited extent. This latter assumption is made in order not to arrive at a completely unreasonable estimate for the available amount of solid particles.

The present work is aimed at determining whether icy grains at the heliocentric distance (r_h) of SW1 could behave in the way required to explain the coma source of CO, and, if so, if their physical properties agree with what has been learned about coma grains from actual observations of comets. Unless noted, all modelling done in this paper was done for $r_h = 6$ AU.

2. Modeling

Icy grains released from the cometary nucleus are assumed to consist primarily of crystalline water ice, containing inclusions of more volatile ices – CO being the species of interest here. It must be possible for the grains to reach temperatures high enough for the water ice to sublimate, thereby also releasing the contained gases. Particles of pure water ice have very long lifetimes (several thousand years) at large heliocentric distances such as that of SW1 (e.g. Lien 1990), while the estimated timescale for gas release in the extended CO source is around a few weeks. The grains must thus incorporate some absorbing agent, for the solar radiation to bring them to a temperature high enough for efficient sublimation to start.

Modelling of water sublimation from grains by previous investigators (Liechtenegger & Kömle 1990) has demonstrated how the grains are eroded, not at a steady rate, but with a very quick sublimation "burst" at the end of the grain lifetime. Their model was run for $r_h = 1$ AU, and treated solid grains of pure water ice, sublimating from the surface. The accelerated behaviour of the grain sublimation is due to the connection between grain size and temperature. As a grain sublimates, its size decreases. This gives the grain a higher temperature which in turn gives a higher sublimation rate.

While solid grains have been studied previously, porous grains are studied here. These have sizes on the order of microns, and are assumed to be effectively isothermal. Sublimation of the ice is occurring not only from the surface, but also from inside the grains. The effective surface area of the porous grains is assumed to be larger than the surface area defined by the grain radius. Instead of a decreasing grain radius, the erosion manifests itself by an increasing porosity of the grains, while their radii are kept constant. The sublimation thus makes the grains increasingly fluffy.

While it is the release of CO that is of interest, it is the evaporation of the enclosing material, water ice, that is treated in the model. The release of CO is assumed to directly follow the H_2O sublimation, and as a simplification, the presence and sublimation of CO does not influence that of H_2O.

2.1. Grain composition

The model used here assumes the grains to be porous, spherical particles. Two types of material are considered.

Material 1 is based on the structure for cometary grains outlined by Greenberg & Hage (1990). The grains are assumed to be aggregates of small three-component particles. This basic building block is a three-layer grain consisting of a silicate core surrounded by an organic component, both covered by a mantle of crystalline water ice. CO and other volatile molecular species are assumed to be embedded in this ice mantle, and sublimation of the H_2O ice is the mechanism assumed to govern their release. These grains are submicron-sized, and larger grains are formed as porous aggregates of the basic grains. The radii r_c and r_o of the two inner layers in the basic grains, as shown in Fig. 1, are set to 0.07 and 0.09 μm, respectively (Li & Greenberg 1997). The radius of the ice mantle is denoted r_i and is used as a model parameter, since it can be used to vary the relative content of absorptive material.

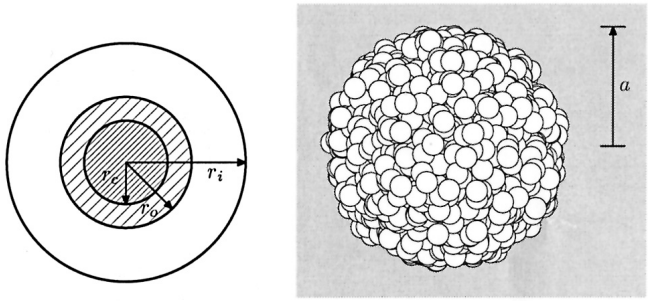

Fig. 1. The structure of the icy grains labelled material 1 (left). Larger particles are formed by spherical aggregates of such basic grains (right).

Refractive indices for the silicates, organics and H_2O ice used in the model were from laboratory data (presented in Li & Greenberg 1997, kindly provided by C. Shen).

These are wavelength-dependent complex parameters given as

$$m = n - ik.$$

The Maxwell-Garnett effective medium theory was used to calculate the effective refractive index m_{av}^i of a core-mantle composite particle (Greenberg & Hage 1990), as

$$(m_{av})^2 = m_1^2\left(1 + 3q^3\left(\frac{m_2^2 - m_1^2}{m_2^2 + 2m_1^2}\right)\left(1 - q^3\left(\frac{m_2^2 - m_1^2}{m_2^2 + 2m_1^2}\right)\right)^{-1}\right)$$

where q is the fractional radius, and m_1, m_2 are the refractive indices of the two components. This was employed twice here to calculate the effective refractive index of the basic grains, first of the silicate core with an organic mantle, and then with an ice mantle added to that, leading to a refractive index m_{bg} of the basic grain. While the structure presented in Fig. 1 is used here in order to present parameters that relate directly to Greenberg's model, the effective medium theory does not take the actual structure into account. How the refractory component is included in the ice does not influence the calculations, which leaves many possibilities open. The refractories could be in numerous smaller particles inside the ice, but also in larger structures that are connected throughout the aggregates. This influences how the grains behave as the ice sublimates. In the former case the refractory component would be lost together with the sublimating ice, while in the latter case only the ice component would disappear, leaving behind porous refractory

grains – a case that would also imply a grain radius unchanged during the sublimation. It is the latter case that is used in the modelling of material 1 presented here.

While pure water ice is used for the ice component in this material, it is the release of CO contained in water ice that is of interest. Whether the CO inclusion influences the optical properties of the ice is not investigated here. CO trapped in water ice has been shown in laboratory experiments to slightly increase the volatility of the ice (Sandford & Allamandola 1988), but this effect occurred at temperatures below 80 K, well below the temperatures of interest here.

Material 2 is a homogeneous mixture of "dirty" ice. This is H_2O ice mixed with ammonia and amorphous carbon. Wavelength-dependent refractive indices (artificial) for this material were taken from Preibisch et al. (1993), where it was presented as representative for icy grains in the interstellar medium. This material is also assumed to consist of basic spherical particles, with $r_i = 0.2\,\mu$m.

For both materials, the refractive index m_p of porous aggregates was calculated using another form of the Maxwell-Garnett formula, as

$$m_p^2 = 1 + \frac{3(1-p)(m_s^2-1)(m_s^2+2)}{1-(1-p)(m_s^2-1)(m_s^2+2)}$$

where p is the porosity and m_s the refractive index of the solid material. For material 1, m_s is the same as m_{bg}.

2.2. Grain temperatures

A key factor to study is the temperature that the coma grains can reach at the heliocentric distance of ∼6 AU where comet SW1 resides. The temperature T of a grain is derived by solving the balance between E_{sol}, the energy received from the Sun, and E_{rad}, the energy reradiated in the infrared. In addition to the energy received from the Sun, three other possible heating mechanisms can be mentioned. These are (1) collisions with gas molecules in the coma, (2) heating by the solar wind, and (3) heating by radiation from the gas, dust and nucleus (Lien 1990). These effects are all assumed to be negligibe with respect to the solar heating since the solar wind is weak and the coma is optically thin in the region that is investigated here. Together with the thermal radiation, cooling by sublimation must also be mentioned. This is given as $E_{subl} = H(T)Q_{H_2O}(T)$, and is the product of the latent heat of sublimation and the H_2O production rate (see Sect. 2.3). However, this term is found to be several orders of magnitude lower than E_{rad} at the temperatures considered here, and is also neglected.

The balance equation $E_{sol} = E_{rad}$ is given by

$$\int_0^\infty \pi a^2 Q_a(\lambda) R(\lambda) \mathrm{d}\lambda = \int_0^\infty \pi a^2 Q_a(\lambda) 4\pi B(T,\lambda) \mathrm{d}\lambda. \quad (1)$$

Here $R(\lambda)$ is the solar flux at 6 AU, approximating the Sun as a blackbody of temperature 5770 K, and $4\pi B(T,\lambda)$ is the Planck function for the grain temperature T. $Q_a(\lambda)$ is the absorption efficiency of the grains. Assuming the porous grains to be perfect spheres, this can be calculated using Mie theory from the refractive index m_p and the size parameter $X = 2\pi a/\lambda$.

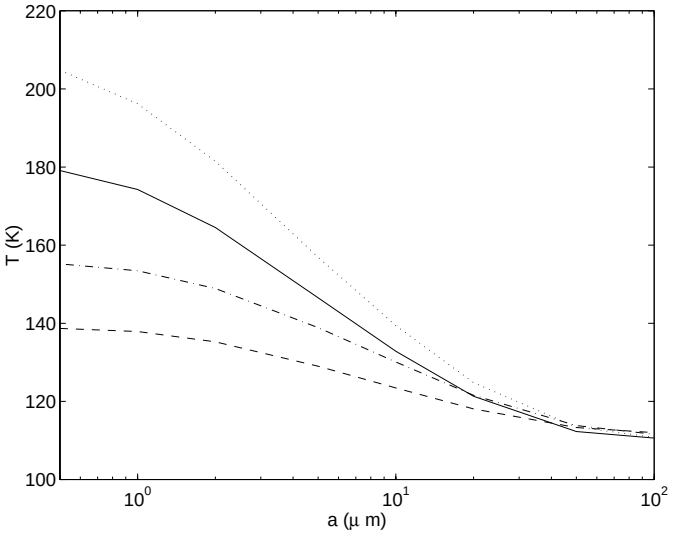

Fig. 2. The equilibrium temperature of grains at $r_h = 6$ AU, as a function of grain radius. Material 1 is shown for $r_i = 0.15\,\mu$m (solid line), $r_i = 0.20\,\mu$m (dash-dotted line), $r_i = 0.25\,\mu$m (dashed line). The temperature for material 2 is shown as a dotted line. The porosity was 0.5 in all cases.

A well-known computer code (Bohren & Huffman 1983) was used to do the calculation of $Q_a(\lambda)$. This code performs the series evaluations involved in the Mie solution and calculates the scattering and extinction coefficients and efficiencies. The absorption efficiency is derived from this as $Q_a = Q_e - Q_s$.

The appearance of Q_a versus λ varies strongly depending on the composition of the grain. Its value is in the range 0 to 1.5, and among the permanent features is a peak at 3 μm, resulting from the content of H_2O ice.

Figure 2 shows the equilibrium temperature as a function of grain radius, with $p = 0.5$. Both materials are shown, and for material 1, three cases of different relative ice content are shown, with $r_i = 0.15$, 0.20 and $0.25\,\mu$m. Similarly, Fig. 3 shows the dependence of equilibrium temperature on the porosity, for a grain radius of $5\,\mu$m. Sublimation of the ice is not included in this calculation, and it should be noted that grains with temperatures above 150 K lose their ice component during just a few minutes after release from the nucleus.

It is clear that the grain radius is a dominating factor controlling the temperature. For effective H_2O sublimation to start, the grains must not be larger than a few tens of microns.

The equilibrium temperature also increases with increasing porosity, a dependency that has been noted also in refractory grains by Greenberg & Li (1998). The choice of material, and relative content of the absorbing agent, has a strong influence on the temperature. This effect dominates over the dependence on porosity.

While this calculation describes equilibrium temperatures without including sublimation of the ice, it should be noted (from Fig. 2) that most grains with radii smaller that a few microns, and a value of r_i smaller than $0.25\,\mu$m, are so hot that they would lose their ice content very quickly.

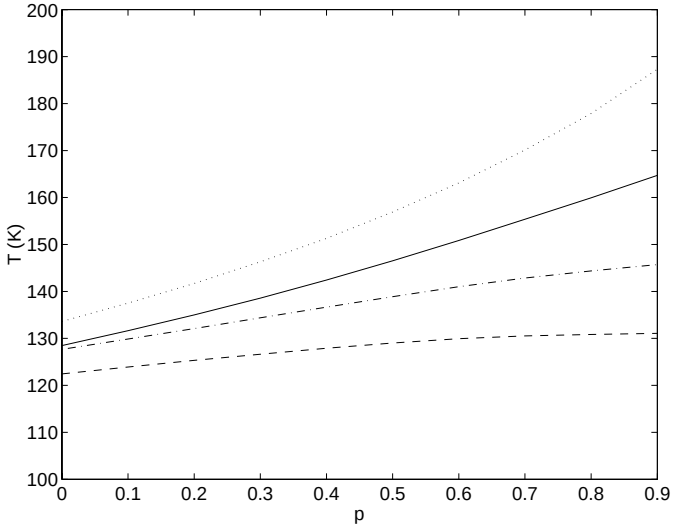

Fig. 3. The equilibrium temperature of grains at $r_h = 6$ AU, as a function of porosity. Material 1 is shown for $r_i = 0.15\,\mu$m (solid line), $r_i = 0.20\,\mu$m (dash-dotted line), $r_i = 0.25\,\mu$m (dashed line). The temperature for material 2 is shown as a dotted line. The grain radius was $5\,\mu$m in all cases.

2.3. Time-dependent grain activity model

A conclusion from Paper II was that the majority of the grains constituting the extended CO source in comet SW1 must have a low activity level upon release from the nucleus, becoming more active after a time delay of order 10^6 s. A time-dependent model for grain sublimation has been constructed to, firstly, investigate whether such a behavior is at all possible and, secondly, try to find limits for the physical properties of the grains.

The model follows a single grain of radius a which is ejected into free space with an initial porosity p_0. The grain then contains a starting mass $m_{\rm ice}^{t=0}$ of H_2O ice, given by

$$m_{\rm ice}^{t=0} = \frac{4\pi a^3 \rho_{\rm ice}}{3} \frac{(r_{\rm i}^3 - r_{\rm o}^3)}{r_{\rm i}^3}(1 - p_0)$$

for material 1, and

$$m_{\rm ice}^{t=0} = \frac{4\pi a^3 \rho_{\rm ice}}{3}(1 - p_0)$$

for material 2. For each timestep in the subsequent evolution, the absorption efficiency $Q_{\rm a}$ must be calculated.

An approximate solution exists for the calculation of $Q_{\rm a}$ (see e.g. McGuire & Hapke 1995), but its validity is limited to wavelengths shorter than the particle size. This is adequate for the absorption and scattering of sunlight, but not for these calculations, since $Q_{\rm a}$ must be accurately calculated also for the wavelength interval where energy is reradiated. Mie theory produces an exact solution to this, but requires a considerable amount of computation. A practical solution is to use a large precalculated table that covers the values of p and a that are of interest. The Mie code was used to calculate $Q_{\rm a}(\lambda)$ once for each point on a grid where p varied from 0 to 1 and a varied from 0.5 to $50\,\mu$m. The resulting 3-D matrix with values for $Q_{\rm a}(\lambda, a, p)$ is used as a large look-up table. For any given values of a and p, the corresponding $Q_{\rm a}(\lambda)$ can then be calculated with adequate accuracy using interpolation in this table.

Using the absorption efficiency, Eq. (1) is solved numerically to calculate the grain temperature.

The temperature determines the H_2O sublimation rate in the grain. Sublimation is assumed to occur throughout the porous material and not only from the surface of the spherical grain. The production rate is given by

$$Q_{\rm H_2O} = 4\pi a^2 S_{\rm A} P_{\rm v}(T) \sqrt{\frac{m_{\rm H_2O}}{2\pi k T}} \quad (2)$$

where $m_{\rm H_2O}$ is the molecular mass. The vapor pressure is calculated as (Liechtenegger & Kömle 1990)

$$P_{\rm v} = P_{\rm r} \exp\left[\frac{m_{\rm H_2O} L}{k}\left(\frac{1}{T_{\rm r}} - \frac{1}{T}\right)\right]$$

where $P_{\rm r} = 10^5\,{\rm N\,m^{-2}}$, $T_{\rm r} = 373\,{\rm K}$ and $L = 2.78 \times 10^6\,{\rm J\,kg^{-1}}$. Equation (2) describes sublimation into vacuum, and assumes all released molecules to escape unimpeded also from pores in the grain.

$S_{\rm A}$ is a correction factor translating the surface area of the grain into the total sublimating area of the porous medium. This factor is calculated on the assumption that the grains consist of small component spheres of radius $r_{\rm i}$. $S_{\rm A}$ is the ratio of the total surface area of the component spheres to the surface area of the grain with radius a. An additional condition applies for small porosities. The minimum porosity possible for packed spheres is $1 - \pi/\sqrt{18}$ (Hales 1997), which must also correspond to the largest possible value of $S_{\rm A}$. If the material is denser than this, there is no room for more small component spheres, and the total surface area must be smaller than that of $p = 1 - \pi/\sqrt{18}$. As a boundary condition, $p = 0$ must give $S_{\rm A} = 1$, since no pores means that only the surface area of the grain is exposed. For values of p smaller than $1 - \pi/\sqrt{18}$ a linear increase in $S_{\rm A}$ is assumed, up to the maximum value, followed by a linear decrease to 0 when p is larger than $1 - \pi/\sqrt{18}$:

$$S_{\rm A} = \frac{a(1-p)}{r_i}; p \geq 1 - \pi/\sqrt{18}$$

$$S_{\rm A} = 1 + \frac{p}{1 - \pi/\sqrt{18}}\left(\frac{\pi a}{\sqrt{18} r_i} - 1\right); p < 1 - \pi/\sqrt{18}.$$

Since the value of $S_{\rm A}$ can be several times unity in some cases, and since the sublimation rate is directly dependent on this factor, the grain lifetimes are quite dependent on how this parameter is calculated. Naturally, this brings some uncertainty into the estimation of grain lifetimes. If an estimate for "sticking" of water molecules to pore walls is introduced, allowing recondensation of released molecules, or if the aggregate has a lesser exposed surface area (smaller $S_{\rm A}$), grain lifetimes would be longer.

The sublimation results in a mass loss

$$\frac{{\rm d}m_{\rm ice}}{{\rm d}t} = -Q_{\rm H_2O} m_{\rm H_2O}$$

which manifests itself as an increasing porosity,

$$\frac{{\rm d}p}{{\rm d}t} = -\frac{{\rm d}m_{\rm ice}}{{\rm d}t} \frac{3}{4\pi a^3 \rho_{\rm ice}}.$$

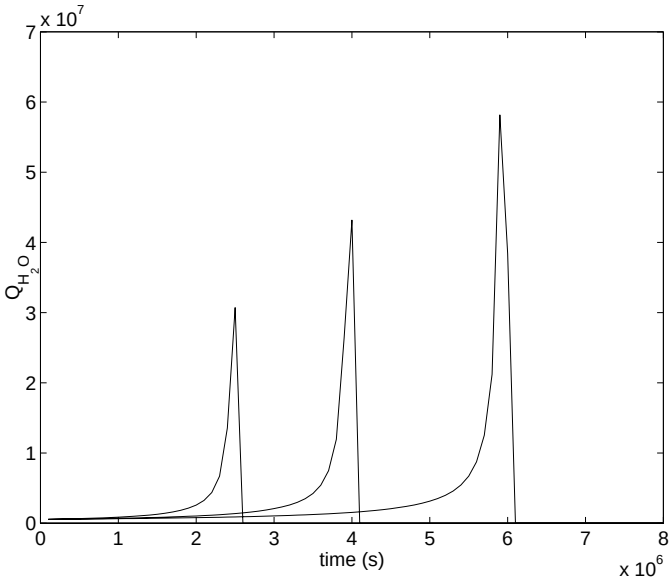

Fig. 4. The sublimation rate Q_{H_2O} as a function of time for three different grain radii, at $r_h = 6$ AU. The graph shows material 1 with with $r_i = 0.25\mu$m and grain radii (counting the peaks from left to right) of 5, 6 and 7 μm. The initial porosity p_0 is 0.5 in all cases.

The above equations provide a complete description of the time-dependent behavior of the icy grains. As a simplification, the erosion of the grains is described by the increasing porosity, while their radius a is kept constant.

Materials 1 and 2 are treated slightly differently in the time-dependent model. The dirty ice constituting Material 2 is viewed as a homogeneous matter, and the pollutants embedded in the ice are released together with the gas as the sublimates. The refractories in material 1, on the other hand, are assumed to stay in the grains as the ice sublimates, thereby altering the relative refractory/ice content. This leads to higher temperatures than those shown in Fig. 3 when p becomes high.

When a grain has exhausted its ice content the sublimation rate becomes zero. It is then removed from the simulation. It is reasonable to assume that the mass loss results in a decreasing with time as well, especially if the refractories are embedded in the ice as discrete particles. The combined effect of decreasing a and increasing p would result in an even more accelerated evaporation of the grains once the sublimation rate has become significant. Given the other uncertainties of the process, only a variable p is treated for now.

Figure 4 shows the sublimation rate from grains with initial porosities $p_0 = 0.5$, but with different radii. Material 1 was used, with an r_i of 0.25 μm. Although the grain radius is constant, it is apparent that the process of grain sublimation has an inherent "avalanche" effect, where most of the ice content sublimates in a short burst at the end of the life of a grain. This happens when the temperature rises above ~150 K. The energy consumed by the sublimation is much lower than what would be needed to significantly slow down the rapid sublimation once started. The burst effect is due to the exponential dependence on temperature of the H_2O sublimation rate. During their life, the temperature of the grains increases as the porosity increases. As the porosity increases, the absorption efficiency decreases in the wavelength interval where the thermal IR radiation from the grain is peaking, while that of the shorter wavelengths where energy is received from the Sun is unchanged. This means that the grain is emitting less energy whilst still absorbing an unchanged amount, which leads to an increase in temperature. A chain reaction is thus at work, which results in the accelerated behavior seen in Fig. 4. Depending on how the initial properties of the grain are chosen, this burst of sublimation can occur at times that are in agreement with the time delay found in Paper II.

Since the porosity p of grains is viewed as a measure of how much ice has sublimated from them, it follows that the initial porosity p_0 also controls the lifetime. The smaller the value of p_0, the longer the lifetime of the grains.

2.4. Grain lifetimes

In order to determine the range of grain sizes and porosities that will lead to a general shell-like extended source profile the lifetime of grains is studied. This lifetime is defined simply as the timestep where the ice content is exhausted. An overview of the lifetime of grains, depending on the model parameters, is shown in Tables 1 and 2. In Table 1, lifetimes for material 1 are shown, for different a and r_i, the latter controlling the amount of ice relative to refractories. The value of p_0 was 0.5 in all cases. In Table 2 lifetimes are shown for material 2, for different a and p_0.

By inspection of Tables 1 and 2 it is clear that lifetimes of order 10^6 s are indeed possible for the types of grains examined. However, for a certain value of p_0 or r_i, only a fraction of a grain population with different grain sizes would fall into the "right" lifetime category.

Since the effect that is to be confirmed requires no or little activity before 10^6 s, Tables 1 and 2 show that grains of material 2, or grains of material 1 with a r_i of 0.24 or less make small grains sublimate too early. These cases would inevitably result in a significant amount of grain sublimation just after release, even if most of the ice mass is contained in larger grains. Removing this effect would call for a grain population devoid of small grains, which is unrealistic.

A central result here is thus that the grains have to be *very icy*, i.e. that they are composed mostly of ices. On the other hand, a very small inclusion of absorptive material, as examplified by the last line of Table 1, where $r_i = 0.30\mu$m, results in low temperatures, and lifetimes of order 10^6 s only for very small grains.

Apart from arriving at lifetimes that agree with the coma source in SW1, the model should also reproduce the absence of a distributed source (due to icy grains) seen in comets closer to the Sun. In particular, the CO prodcution in comet Hale-Bopp was shown not to be of extended nature when at 2 AU from the Sun (DiSanti et al. 1999). Figure 5 shows the lifetimes for grains of material 1, with $r_i = 0.28\mu$m and $p_0 = 0.5$ for four different grain radii.

Inside 3 AU from the Sun, the grains lose their icy component quickly, making grain activity indiscernible from nuclear outgassing.

Table 1. The lifetimes (10^5 s) of grains of material 1 with varying r_i and a, and with $p_0 = 0.50$.

	a (μm)								
r_i	1	2	3	5	7	10	20	30	50
0.16	< 1	< 1	< 1	< 1	1	7	>200	>200	>200
0.18	< 1	< 1	< 1	1	2	8	>200	>200	>200
0.20	< 1	< 1	< 1	2	4	14	>200	>200	>200
0.22	< 1	1	1	4	10	32	>200	>200	>200
0.24	1	2	4	13	31	88	>200	>200	>200
0.26	4	9	16	48	113	>200	>200	>200	>200
0.28	18	37	69	199	>200	>200	>200	>200	>200
0.30	78	165	>200	>200	>200	200	>200	>200	>200

Table 2. The lifetimes (10^5 s) of grains of material 2 for different p_0 and a.

	Grain radius (μm)								
p_0	1	2	3	5	7	10	20	30	50
0.1	<1	<1	1	18	>200	>200	>200	>200	>200
0.3	<1	<1	<1	2	20	>200	>200	>200	>200
0.5	<1	<1	<1	<1	2	12	>200	>200	>200
0.7	<1	<1	<1	<1	<1	1	16	173	>200
0.9	<1	<1	<1	<1	<1	<1	<1	<1	3

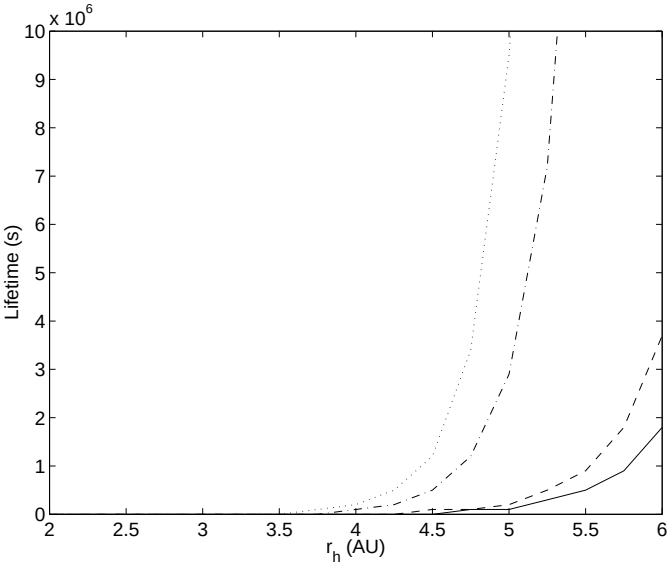

Fig. 5. Lifetimes for grains of material 1, for different r_h. Here r_i = 0.28 μm, and p_0 = 0.5. The four lines show a = 1 μm (solid line), a = 2 μm (dashed line), a = 10 μm (dash-dotted line) and a = 20 μm (dotted line).

2.5. Grains with a size distribution

Two ideas are suggested for how a population of grains of a "real" size distribution could produce a total activity peaking just after a time of order 10^6 s: (1) The initial porosity of the grains could depend on the grain size, making larger grains more porous than smaller ones, giving similar lifetimes to grains of different sizes. (2) A significant ice mass could reside in very small grains. Here, it is assumed that a large amount of grains with grain diameters under 6 μm are present.

The grain sublimation model is used to create a radial activity profile of the extended source. Model runs have been made for a number of test grains, and the results are added together to generate a plot of the total activity in the grains versus time.

The test grains have a power-law size distribution:

$$n(a)\mathrm{d}a = \begin{cases} N_0 a^{-\beta}\mathrm{d}a & ; \ a_{\min} < a < a_{\max} \\ 0 & ; \ \text{otherwise.} \end{cases}$$

For the idea of a size-dependent grain porosity, there should be a relationship for the variation of p_0 for different grain radii. A dust density dependent on a has been used by e.g. Lamy et al. (1987) to analyse Giotto data, allowing the density of refractory dust grains to be a factor of ~2 larger for a = 1 μm than for a = 10 μm. Laboratory experiments simulating the accumulation and structure of cometary material have shown that a dependence of this character should exist (Donn 1991). The density of fractal-structured particles does indeed drop as a function of their size, as $\rho \propto a^{D-3}$, where D is the fractal dimension.

Applying an a-dependent porosity for the test grains in the sublimation model presented here shows that a grain population spanning a certain range of sizes can produce a production profile that initially maintains a low activity level, but where most of the sublimation occurs in an activity peak of relatively short duration.

However, this approach imposes a strict requirement on the porosity, which appears a bit unrealistic. Also, larger grains would have to be extremely fluffy to get a lifetime similar to that of micron-sized grains, a property that must then also apply to the bulk nuclear material.

In the second approach the ice mass is concentrated in small grains, or at least, a significant amount of ice is released as small grains. A fixed initial porosity is assigned. From Table 1 it is seen that, for p_0 = 0.5 and r_i = 0.28 μm, the lifetimes are

of order 10^6 s for grains with $a < 5\,\mu$m. Figure 6 shows an activity profile for one kilogram of material 1, where only small grains are included ($0.5 < a < 3\,\mu$m), and with a p_0 of 0.45 and a β of 4.5. While no large grains are included in the run, they are not assumed to be absent, but they have temperatures too low to make an impression on the activity profile. This model produces a pronounced activity maximum at 2×10^6 s after release, which is what is sought. A few small discontinuities that appear in the shape of the profile after the maximum are sampling effects caused by the limited number of test particles. Of the total ice mass, 91% is left to sublimate after 10^6 s, and 70% sublimates between 10^6 s and 4×10^6 s.

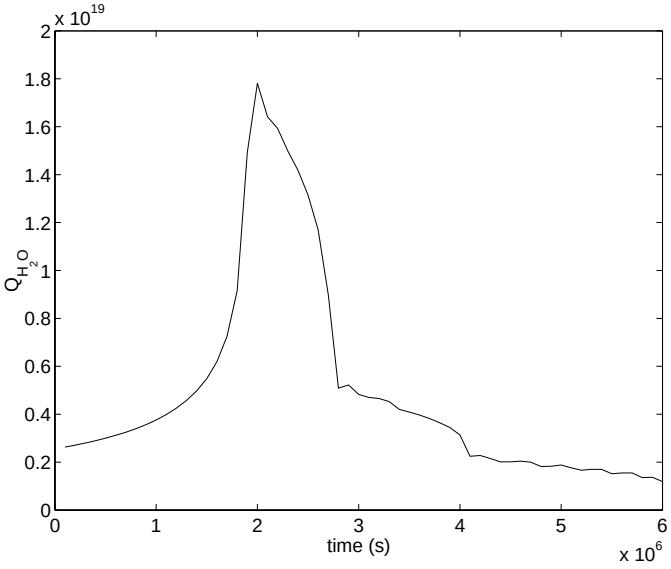

Fig. 6. The total sublimation rate Q_{H_2O} from 1 kilogram of grains of material 1, as a function of time, where $r_i = 0.28\,\mu$m, $a_{min} = 0.5\,\mu$m, $a_{max} = 3\,\mu$m, and $p_0 = 0.5$. β was set to 4.5.

2.6. Fragmentation

Starting from the assumption that all grains have a similar initial porosity around 0.5 it is readily seen, in Tables 1 and 2, that grains larger than $\sim 10\,\mu$m will be effectively inactive in the timeframe discussed here. If there is no large population of small icy grains ejected from the nucleus, as suggested in the previous section, and most of the total ice mass is contained in larger grains ($\beta < 4$), this means that the icy dust output of the comet will remain inactive long enough for the dust coma to disperse and only a small fraction will sublimate in the "right" timeframe.

This dilemma could be solved if the idea of *fragmentation* is introduced. If a large grain is split into smaller pieces, material constituting the large inactive grain could be moved to the domain where $a < 5\,\mu$m. Then, the new radii of the fragments allow for quick sublimation of the ice. Such an effect would dominate over the time-dependent thermal evolution modeled in this work.

The idea of fragmentation is introduced in the model using a very simplified assumtion and only one additional model

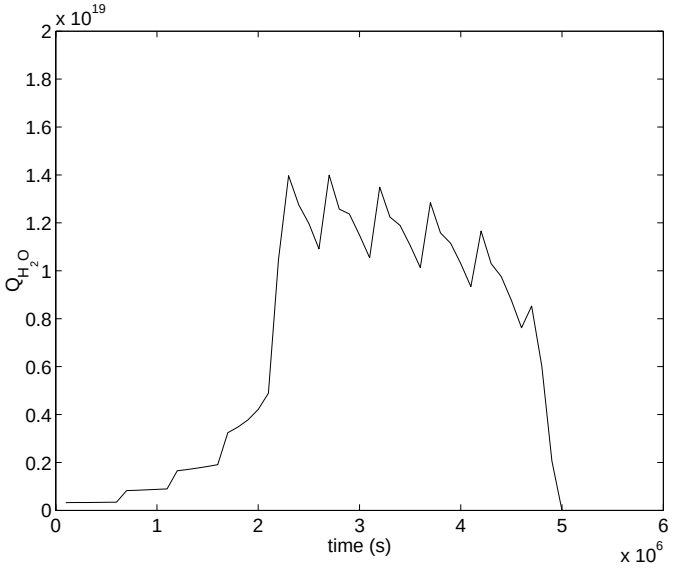

Fig. 7. The total sublimation rate Q_{H_2O} from 1 kilogram of grains of material 1, as a function of time, where $r_i = 0.28\,\mu$m, $a_{min} = 1\,\mu$m, $a_{max} = 40\,\mu$m, and $p_0 = 0.5$. β was set to 4.0. Fragmentation of the grains is occurring on a timescale $t_f = 5 \times 10^5$ s.

parameter, the fragmentation timescale t_f. When the time t_f has passed, a grain of radius a breaks up into eight (spherical) pieces of radius $a/2$. All grains will become small enough to sublimate when a number of fragmentation cycles have passed.

Figure 7 shows a model run using fragmentation. The timescale t_f was set to 5×10^5 s, and the size distribution was described by $a_{min} = 1\,\mu$m, $a_{max} = 40\,\mu$m, and $\beta = 4.0$. The "boxy" activity region results when the smallest grains become active first, and grains descending from larger grains become active after consecutive fragmentation cycles. The jagged appearance of the profile is an effect of the simple assumption of a single t_f. The "bumps" result from consecutive generations of fragmentation. Since all initial grain sizes contribute the same amount of mass, the process appears to smear out the activity in time. However, the profile still displays the characteristics of the extended source activity, with all sublimation occurring in a limited region.

Figure 8 shows a model run using the same parameters as in Fig. 7, but with $\beta = 3.3$, as found by Fulle (1992). This size distribution puts more mass in larger grains, and as fragmentation progresses, an increasing amount of material arrives at sizes small enough to sublimate. This leads to the gradual increase seen in the shape of the profile. The activity is terminated when the population (initially limited at $40\,\mu$m) is exhausted. Naturally, this is expected also in reality since there must be some limit to the available amount of larger grains. The activity profile should display a maximum, followed by a gradual decrease as the population of larger grains is depleted.

Fragmentation was observed to occur for refractory grains in comet Halley (Eberhardt et al. 1987). Fragmentation of grains is also suggested in the case of comet Hale-Bopp (DiSanti et al. 2001) to explain the strong increase in production of micrometre-sized dust observed with decreasing heliocentric distance, as compared to that of larger,

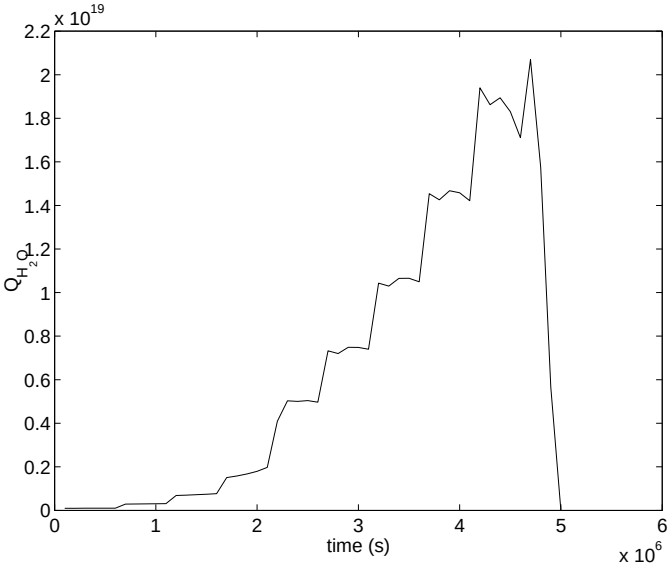

Fig. 8. The total sublimation rate Q_{H_2O}, using the same parameters as in Fig. 7, but with β set to 3.3.

millimetre-sized dust grains. The process of grain fragmentation is also suggested to be at play in most comets observed from the ground, in order to explain the shape of the isophotes in the dust coma (Combi 1994). Here, however, splitting is proposed at $r_h = 6$ AU for grains with a significant ice component.

For the question of what causes the fragmentation, it has been suggested that it is due to dust acceleration by the nuclear outgassing (Combi 1994), but for SW1, the acceleration should be effective only in the innermost coma. It remains to find a real physical description of the process behind the splitting of icy grains, especially for those that are too cold for water sublimation to be efficient.

3. Discussion

The main objective of this study has been to determine if the characteristics of the extended source, that were outlined from the results in paper II, could be reproduced by a simulation modeling actual icy grains at this heliocentric distance. This has been shown to be a real possibility, but the results rely on model parameters, for which the real counterparts are largely unknown. Depending on the structure of the grains, the amount of absorbing material in the water ice, the size distribution etcetera, the quantitative results may vary strongly.

It is natural to make a comparison with comet Hale-Bopp. This comet has displayed several similarities to SW1, in the sense that they both have large nuclei (tens of km across) and both have displyed CO-driven activity at large r_h, with strikingly similar outgassing patterns. Observational evidence for icy grains in the coma of comet Hale-Bopp was found in ISO observations, where the H_2O ice features at 3.1, 44 and 65 μm were detected (Lellouch et al. 1998). The comet was then at a heliocentric distance of 2.9 AU, far enough for the grains not to sublimate directly upon release. The grains in the coma of comet Hale-Bopp were estimated to have mean radii of 15 μm, and lifetimes around 2 days. Using the model presented here with $r_h = 2.9$ AU such lifetimes can be reproduced by material 1 for very icy grains, with r_i around 0.3 μm, and but not by material 2.

If comet Hale-Bopp is similar to SW1, as suspected, this would suggest that the material constituting the icy grains could be described as material 1 treated here. The observations of comet Hale-Bopp were made on the pre-perihelion branch of the orbit, when the H_2O sublimation rate was around 4×10^{29} s^{-1}.

The only known constraint for the extended source activity at 6 AU is that a low total activity level is required before 2–4×10^6 s after grain release. An additional constraint is given by the fact that a very large and diluted source would require unreasonably large amounts of grains to give the observed results. Therefore, a limited activity profile, with a maximum just after 2×10^6 s has been sought.

A peaked activity profile could be produced by grains of a population arranged so that larger members are more porous, giving all grains similar lifetimes. However, in the model presented here, such a size-dependent porosity would have to be very precisely defined and fine-tuned for this effect to appear. Also, the required porosity for larger grains would be very high, which limits the size range where this idea could be used. Though the idea of a size-dependent porosity of the icy grains is certainly not ruled out, it apparently cannot provide a complete explanation for the extended source structure.

It is perhaps more realistic to assume that a large amount of small grains are available, as such a population always produces a peaked extended source activity profile, the position of which is defined by the limiting smallest grain size. The porosity of the ice would not have to be so fine-tuned, but the grains should be fairly dense, with a p_0 of 0.5 or lower.

A main result from this work is that the grains must be very icy, containing only a small volume fraction of refractory material. There are a number of model parameters influencing the results, and the model may exaggerate the efficiency of sublimation. Including the effect of gas molecules recondensing to the material, or assuming a lesser total surface area of the porous ice would lead to longer lifetimes of the grains, which also means that a smaller ice fraction would be needed for similar lifetimes.

For the grains investigated here, the refractory to ice mass ratio is small, with values in the range 0.10–0.30, assuming a density of 3 g/cm^3 for the solid refractories. While this does not agree very well with the 1:1 dust/gas ratio measured in comets closer to the Sun, those measurements are made when other phenomena may be at work, such as the expulsion of parts of a dust mantle.

The most icy of the grains studied here are initially fairly dense, with $p \simeq 0.5$, but when the ice sublimates the refractory material is left behind as a porous 'skeleton'. The initial volume ratio of the dust and ice components then gives a porosity of around 0.95 for the refractory grains left behind when the ice content is exhausted, which is not far from the value of 0.975 derived for refractory grains in comet 1P/Halley as well as comet Hale-Bopp (Li & Greenberg 1998; Greenberg & Li 1998) at smaller heliocentric distances where the ice has been quickly sublimated before the grains were observed.

A problem when explaining the extended source activity found in SW1 is the large amount of solid material that has to be available to generate the observed CO production rate. The dust mass output derived from observations of SW1 (Fulle 1992) is actually lower than the observed CO output from the extended source. In the dust measurement, a β of 3.3 was used, which puts most of the mass in large grains. This calculation was based on an optical image containing information about grains down to a diameter of 5 μm. This leaves the possibility open for a large amount of smaller grains as proposed here. Comet Hale-Bopp, which is viewed as an object similar to SW1, was observed when at 4.5 AU from the Sun to have a substantial dust output (with icy grains present) of 3×10^4 kg s^{-1} and a large dust to gas mass ratio of up to 10 (Grün et al. 2001). Roughly extrapolating this to SW1 makes the observed CO production rate from grains less unreasonable, if the CO content of the grains is significant. A CO content in excess of 10% is unlikely, but a value close to this limit may be assumed. The large dust to gas mass ratio for a CO-driven comet means that the expulsion of solid particles is very efficient, which is just what is 'needed' for SW1. It appears reasonable that these particles are icy grains, which at smaller r_h would sublimate and bring the dust/gas ratio closer to unity, which is the commonly adopted composition for comets.

While one of the main conclusions from paper II was that the extended source resides in a region at a certain distance from the nucleus, two explanations for this structure were discussed. The first was the thermal delay process that has been investigated here, and the second was the possibility of an outburst having occurred some time before the observations, resulting in an expanding, hollow shell of active grains. However, if the grain population was fully active upon release, outbursts occurring at irregular intervals would have manifested themselves in the many CO spectra recorded for the comet at different times (Biver 1997; Festou et al. 2000). This is not seen, as the shape of the emission line is stable over time. While neither explanation can be ruled out, it is not impossible that both processes are at play at the same time, i.e. whether or not the comet is in outburst, the time delay is probably always present.

Future theoretical work investigating the activity of comet SW1 would incorporate modelling of the nucleus itself. In particular, CO release through crystallization of amorphous ice near the surface, and the expulsion of solid material due to this activity should be studied.

References

Bar-Nun, A., & Kleinfeld, I. 1989, Icarus, 80, 243
Biver, N. 1997, Ph.D. Thesis, Université Paris VII
Bohren, C. F., & Huffman, D. R. 1983, Absorption and scattering of light by small particles (Wiley, New York), Appx. A
Combi, M. R. 1994, AJ, 108, 304
DiSanti, M. A., Mumma, M. J., Russo, N. D., & Magee-Sauer, K. 2001, Icarus, 153, 361
DiSanti, M. A., Mumma, M. J., Russo, N. D., et al. 1999, Nature, 399, 662
Donn, B. 1991, in Comets in the post-Halley era, Vol 1, 535
Eberhardt, P., Krankowsky, D., Schulte, W., et al. 1987, A&A, 187, 481
Festou, M. C., Gunnarsson, M., Winnberg, A., Rickman, H., & Tancredi, G. 2000, Icarus, 150, 140
Fulle, M. 1992, Nature, 359, 42
Greenberg, J. M., & Hage, J. I. 1990, ApJ, 361, 260
Greenberg, J. M., & Li, A. 1998, A&A, 126, 170
Grün, E., Hanner, M. S., Peschke, S. B., et al. 2001, A&A, 377, 1098
Gunnarsson, M., Rickman, H., Festou, M. C., Winnberg, A., & Tancredi, G. 2002, Icarus, 157, 309
Hales, T. C. 1997, Discrete and computational geometry, 17, 1
Hanner, M. S. 1981, Icarus, 47, 342
Lamy, P. L., Grün, E., & Perrin, J. M. 1987, A&A, 187, 767
Lellouch, E., Crovisier, J., Lim, T., et al. 1998, A&A, 339, L9
Li, A., & Greenberg, M. 1997, A&A, 323, 566
Li, A., & Greenberg, M. 1998, ApJ, 498, L83
Liechtenegger, H. I. M., & Kömle, N. I. 1990, Icarus, 90, 319
Lien, D. J. 1990, ApJ, 355, 680
McGuire, A. F., & Hapke, B. W. 1995, Icarus, 113, 134
Preibisch, T., Ossenkopf, V., Yorke, H. W., & Henning, T. 1993, A&A, 279, 577
Sandford, S. A., & Allamandola, L. J. 1988, Icarus, 76, 201